Proceedings Paper:
Porumbel, I., Cuciumita, C.F., Nechifor, C. et al. (2018) Experimental measurements in Hartman oscillators. In: Gherman, B. and Porumbel, I., (eds.) Transportation Research Procedia. 6th CEAS Air & Space Conference Aerospace Europe 2017, 16-20 Oct 2017, Bucharest, Romania. Elsevier, pp. 339-355. ISSN: 2352-1465. EISSN: 2352-1465.

https://doi.org/10.1016/j.trpro.2018.02.031

Available online at www.sciencedirect.com

ScienceDirect

Transportation Research Procedia 29 (2018) 339–355

Transportation Research Procedia

www.elsevier.com/locate/procedia

6th CEAS AIR & SPACE CONFERENCE AEROSPACE EUROPE 2017, CEAS 2017, 16-20 October 2017, Bucharest, Romania

Experimental measurements in Hartman oscillators

Ionut Porumbel[a*], Cleopatra Florentina Cuciumita[a], Cristian Nechifor[a], Radu Kuncser[a], Tudor Cuciuc[b]

[a]*Romanian Research and Development Institute for Gas Turbine COMOTI, 220D, Iuliu Maniu Blvd, Sector 6, Bucharest 061126, Romania*
[b]*Institute for Applied Physics, 5, Academiei St., Chisinau, Republic of Moldova*

Abstract

The paper presents high frequency pointwise measurements of pressure and temperature carried out on a shock wave generator consisting of a couple of supersonic jets impinging on a Hartman oscillator system. The shock wave generator was developed as a means to achieve an aerodynamically controlled pulsed detonation chamber. The analysis allows the selection of the optimal geometry and inlet conditions for such an application. The effect of the inlet conditions and of the geometry of the experimental model on the frequency and amplitude of the pressure waves occurring in the system is analyzed. The paper also presents the effects of other geometrical parameters: the critical section of the jet nozzles, the volume ratio of the resonator geometry, and the inlet angles of the jets. Effects of inlet pressure and temperature are also included.

Peer-review under responsibility of the scientific committee of the 6th CEAS Air & Space Conference Aerospace Europe 2017.

Keywords: detonation; supersonic propulsion; Hartmann oscillators; high frequency measurements.

1. Introduction

The experimental work presented in this paper aimed at developing a high operating frequency detonation chamber. To ensure the correct air flow through the combustor, the classical Pulse Detonation Chamber (PDC) design uses a set of valves that open and close the admission of the air, or air-fuel mixture, in the combustor. The main problem in this approach is the high wear experienced by the valves, even more so at high frequencies. Supplementary, the valves are subject to very high operating temperatures, and will induce pressure losses in the

* Corresponding author. Tel.: +4-072-009-0775; fax: +4-021-434-0241.
E-mail address: ionut.porumbel@comoti.ro

2352-1465
Peer-review under responsibility of the scientific committee of the 6th CEAS Air & Space Conference Aerospace Europe 2017.
10.1016/j.trpro.2018.02.031

flow. To allow significantly higher operating frequencies, up to 1000 Hz, a valveless design, based on carefully timed pressure gradients in the flow, is an obvious goal for research and development. The studied concept uses a high frequency shock wave system to play the role of an aerodynamic valve at the combustor inlet. The shock waves are generated by a couple of supersonic jets impinging on a Hartman oscillator system (Hartmann, 1919 and Hartmann, 1939). The Hartmann oscillator is an acoustic wave generator driven by shock wave oscillations in an over-expanded air jet (Morch, 1964). The Mach disk occurring in the supersonic jet downstream of the nozzle is forced to oscillate in the jet axial direction in the presence of a cavity aligned with the jet flow direction and placed in a bluff body placed downstream of the supersonic jet nozzle. Usually, the bluff body is placed near the end of the first cell of the supersonic jet pattern. Planar supersonic jets were chosen instead of round jets in order to further increase the oscillation frequency (Morch, 1964) . Experimental investigations of such systems, by Morch (1964) and Smith and Powell (1964) date back from the mid XX century, and numerous studies and review papers have been published to the date. A review of the self - induced flow oscillations occurring in supersonic flows, and of the underlying physical mechanisms, was published, for the early research work, by Jungowski (1975). In the more recent years, the focus of the research efforts in the field of self - sustained oscillations induced by Hartmann resonators shifted more to the application of the effect in various flow control solutions. Experimental measurements on supersonic jets impinging Hartmann resonators were reported by Sarohia and Back (1979), Sobieraj and Szumowsky (1991), Kastner and Samimy (2002), Samimy et al. (2002), Raman et al. (2004), Raghu and Raman (1999), Gregory (2005), Sreejith et al. (2008) and Sarpotdar et al. (2005).

The paper is part of a larger study on PDCs based on Hartmann oscillators, including both theoretical considerations (Cuciuc et al., 2017) and numerical studies (Porumbel et al., 2017). Detailed high frequency measurements of pressures and temperatures in selected configurations of a PDC experimental model are presented, aiming at evaluating the candidate solutions and at selecting the best configuration.

The effect of several parameters on the performances of the experimental model is analyzed:

- the inlet total pressure;
- the inlet temperature;
- the size of the minimum section of the convergent – divergent nozzle;
- the distance between the nozzles exits and the resonator sharp edges;
- the angle of the incoming jet with respect to the experimental model centerline was studied.

2. Experimental setup

2.1. Model geometry

The geometry of experimental model is shown in Fig. 1, and dimensional details are given by Cuciuc et al. (207). Location of experimental probes is given in Fig. 3.

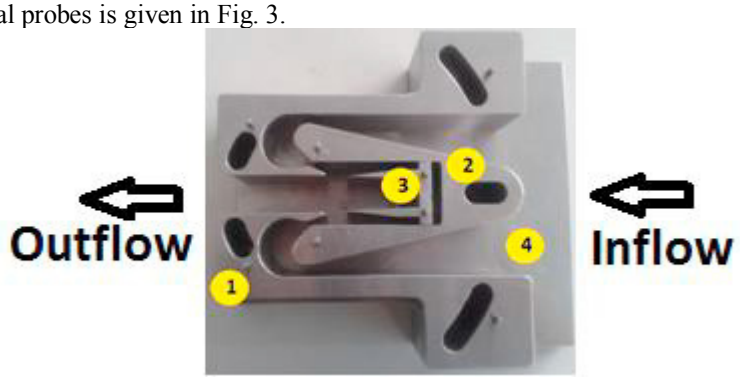

Fig. 1. Experimental model geometry.

The model has four components: the semi-casings (1), the central detonation chamber (2), the resonator (3) and the lateral walls (4), and includes three adjustable geometrical parameters:

- The supersonic nozzle exit angle can be modified by rotating the semi-casings (1) on the lateral walls (4). The center of rotation is selected such that the critical section of the nozzle is maintained constant;
- The distance between the supersonic nozzles exit and the sharp edges of the detonator can be modified by translating the resonator (3) on the lateral walls (4);
- The area of the critical section of the supersonic nozzles can be modified by translating the detonation chamber (2) on the lateral walls.

2.2. Test rig

The diagram of the test rig is presented in Fig. 2. The primary test rig air, provided by the test rig compressor, is fed through a calibration vane into the test rig combustor and the exhaust gas is evacuated, through a pressure control vane, into the test rig exhaust. The exhaust gas temperature is controlled through the mass flow rate passing through combustor, by means of the calibration vane and the pressure control vane, as well as through the fuel mass flow rate passing through the fuel regulation vane. A secondary air line is be pressurized by means of a volumetric compressor, the pressure being controlled by means of a pressure reduction. The total pressure is verified immediately upstream of the experimental model, such that the reduction controls can be set to ensure the desired total pressure can be set to the desired value. The secondary air flows around the combustor and is heated by it to the desired temperature, verified by means of a temperature gauge placed immediately upstream of the experimental model. After passing through the experimental model , the air is directed into the same test rig exhaust.

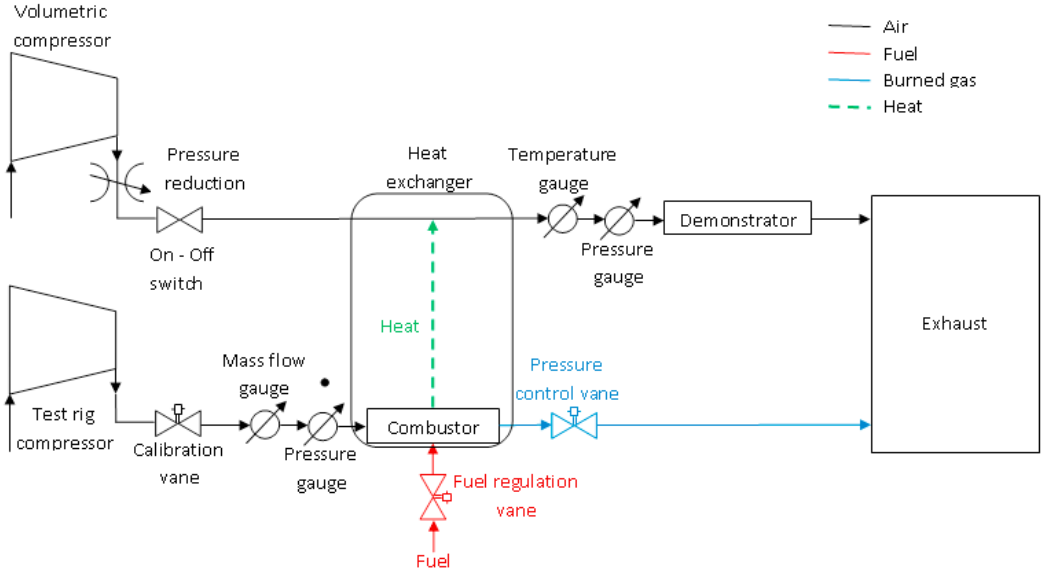

Fig. 2. Test rig layout.

2.3. Measurement points

High speed, point-wise measurements of pressure and temperature were recorded in the positions presented in Fig. 3.

2.4. Instrumentation

For the purpose of the experimental measurements presented here, the following sensors were used:

- Temperature: Coaxial Thermocouple MCT 19; Article number: 100-001-1. Type E; Manufacturer: Muller Instruments; Temperature range: 0 - 1200 K.
- Pressure: Pressure Transducers Types ETM-HT-375M-35BARA and ETM-HT-375M-50BARA; Manufacturer: Kulite; Pressure range: 35 respectively 50 bar.

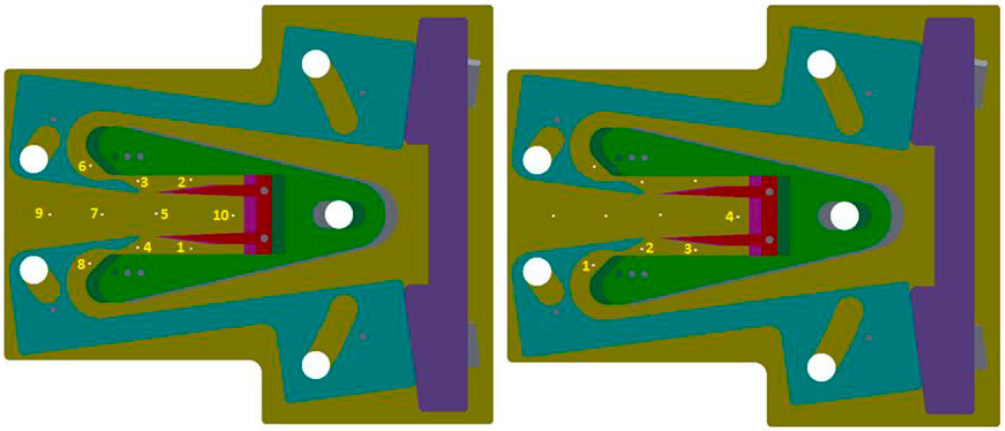

Fig. 3. Sensors layout: pressure (left) and temperature (right).

3. Results and discussion

3.1. Baseline configuration

The tests were carried out with under the following conditions:

- Inlet total pressure:607978 Pa (6.000 bar);
- Inlet static pressure: 524842 Pa (5.180 bar);
- Inlet total temperature: 291.53 K (18.37 °C);
- Mass flow rate: 0.797 kg/s;
- Outlet pressure: 102165 Pa (1.008 bar);
- Outlet temperature: 291.09 K (17.94 °C);
- Critical section: 110 mm;
- Distance from nozzles to resonator: 12 mm.

The pressure and temperature variations in time are presented, respectively, in Fig. 4 and Fig. 5a. The static pressure decreases strongly through the Laval nozzle, from the upstream position 8 to the downstream position 4, indicating a strong acceleration through the convergent – divergent nozzle, characteristic to a supersonic flow. The amplitude of the high frequency oscillations remains the same, of about 20,000 Pa through the nozzle. The low frequency oscillations have lower amplitudes in position 8 (30,000 Pa) than in position 4 (50,000 Pa), as the critical section of the nozzle dampens the oscillations propagating upstream. Further downstream, in the resonator corresponding to the same inlet as for positions 8 and 4, the pressure signal in position 1 indicates slightly lower static pressure values, showing an increase in velocity in the PDC lateral resonator. The amplitude of the low frequency pressure oscillations remains high, in the range of 50,000 Pa, as pressure waves are propagating from the nozzle exit through the resonator. The pressure signal in the opposite resonator, position 2, is in phase to the

pressure signal in position 1, in correlation with the numerical simulations (Porumbel et al., 2017, Porumbel et al. 2014). In general, the two resonator signals are similar. In the central detonation chamber, the pressure signal at position 10 presents significantly lower amplitudes, and is in opposition of phase compared to the signals acquired from the two resonators. The mean pressure value is about the same as inside the resonators. Further downstream, in the central detonation chamber, in position 7, the static pressure mean value decreases substantially, below the atmospheric value, indicating a high velocity in the supersonic jet exiting the PDC. Both the frequency and the amplitude of the pressure oscillations remain similar to those recorded upstream, in position 10.

Fig. 4. Pressure signal for baseline configuration.

The temperature rise due to shock waves in the PDC is of about 15 K. This is insufficient for Hydrogen self ignition, and it will have to be addressed by either raising the inlet temperature and pressure, or by altering the experimental model geometry.

3.2. Effect of inlet pressure

The geometry was unchanged, and the tests were carried out under the conditions in Table 1.

Table 1. Test conditions for evaluating the effect of the inlet pressure.

Test	A		B	
Inlet total pressure [Pa] / [bar]	506633	5.000	709862	7.006
Inlet static pressure [Pa] / [bar]	435864	4.302	613118	6.051
Inlet total temperature [K] / [°C]	291.18	18.03	291.74	18.59

Mass flow rate [kg/s]	0.656		0.928	
Outlet pressure [Pa] / [bar]	102153	1.008	102187	1.008
Outlet temperature [K] / [°C]	289.51	16.36	293.92	20.77

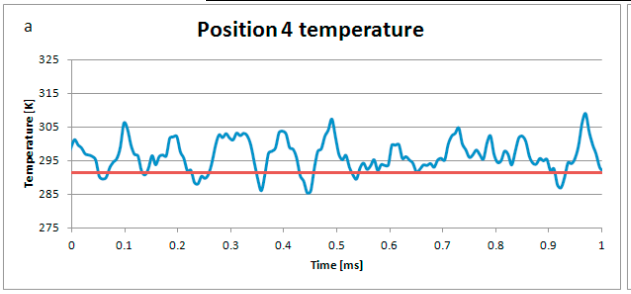

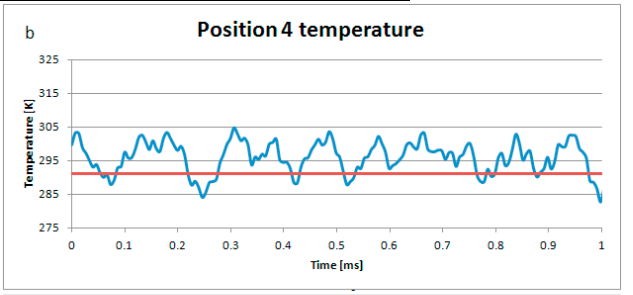

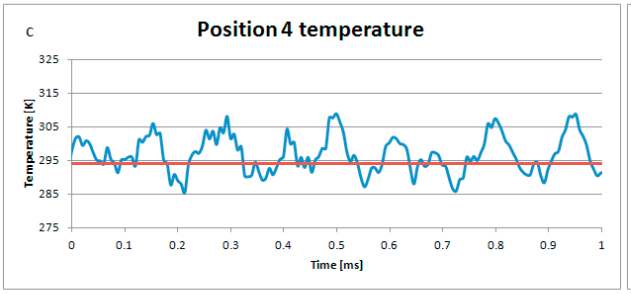

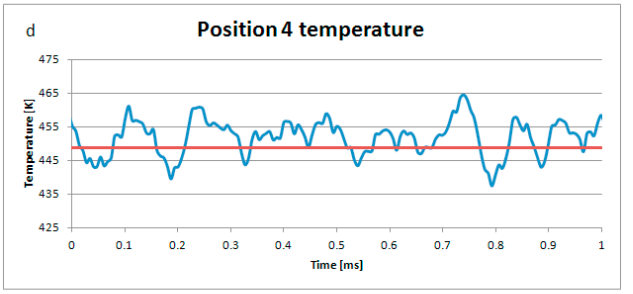

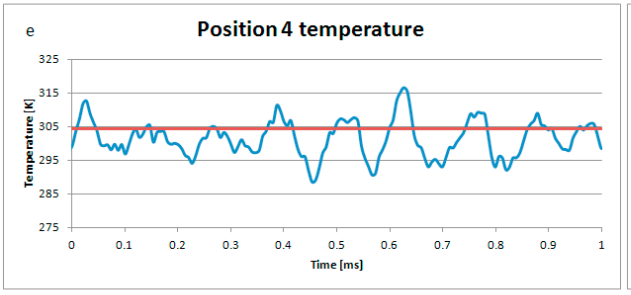

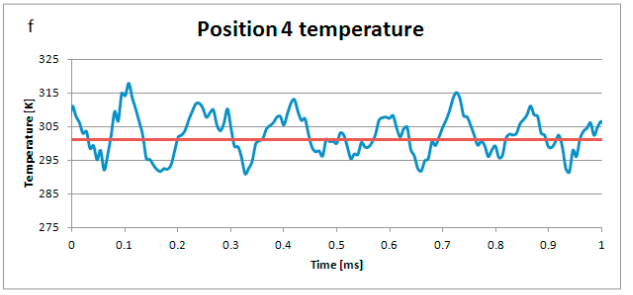

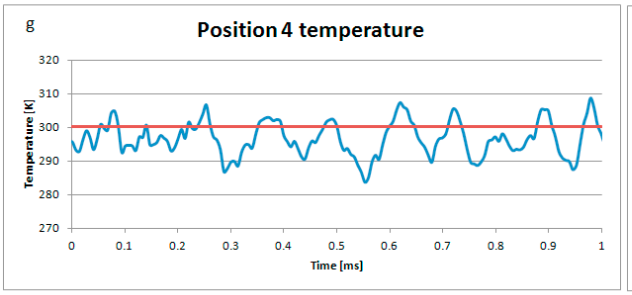

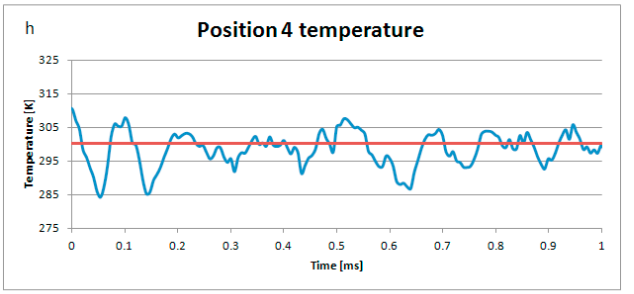

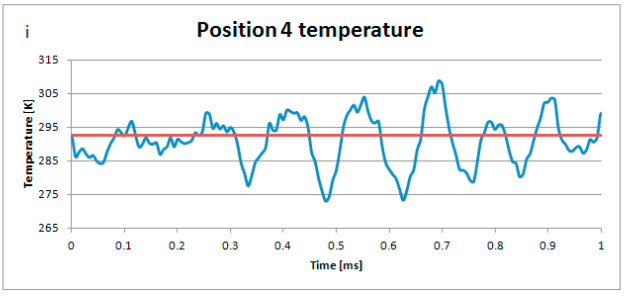

Fig. 5: Temperature signal for: (a) baseline; (b) decreased pressure; (c) increased pressure; (d) increased temperature; (e) decreased critical section; (f) increased critical section; (g) decreased distance to resonator; (h) increased distance to resonator; (i) increased jet angle. The red line indicates the inlet temperature

3.2.1. Case A - Decreased pressure

The pressure and temperature variations in time are presented, respectively, in Fig. 6 and Fig. 5b. Obviously, the static pressures are all lower for this case, because the inlet total pressure was lower. The decrease in static pressure from the upstream position 8 to the downstream position 4 is lower in this case, but remains significant, confirming the strong acceleration through the Laval nozzle to supersonic values. The amplitudes of the oscillations in both positions are smaller, but the low frequency oscillations continue to have lower amplitudes in position 8 than in position 4.

In position 1, the static pressure remains slightly lower than in position 4, due to the decrease in velocity induced in supersonic flow by a convergent channel, but the amplitude of the oscillations is lower than in the baseline case, of about 40,000 Pa. In the other side resonator, the probe in position 2, is still in phase to the pressure signal in position 1, and the two signals coming from the resonators remain generally similar. In the central detonation chamber, the pressure signal at position 10 is again of lower amplitude, but the signal is now in phase with the signal in the two resonators. Downstream, at the PDC outlet, in position 7, the static pressure mean value is about the same as in the baseline case. Since the inlet total pressure is lower in this case, and the geometry, and, hence, the losses are identical, it results that the Mach number at the PDC outlet is now lower than in the baseline case. Neither the frequency, nor the amplitude of the pressure oscillations changes significantly in comparison to the baseline case.

The temperature rise due to shock waves in the PDC is lower in this case than in the baseline case, due to the lower intensity of the shock waves propagating through the PDC.

Fig. 6. Pressure signal for baseline configuration under decreased inlet pressure.

3.2.2. Case B - Increased pressure

The pressure and temperature variations in time are presented, respectively, in Fig. 7 and Fig. 5c. Obviously, the static pressures are all higher, because the higher inlet total pressure. The decrease in static pressure from the upstream position 8 to the downstream position 4 is higher than in the baseline case, due to the supersonic acceleration in the Laval nozzle. In both positions, the amplitudes of the oscillations are higher than in the baseline case, and with lower amplitudes for the low frequency oscillations at the nozzle exit, in position 4, than at its inlet, in position 8. In position 1, the static pressure is lower, as the velocity decrease in the resonator convergent channel is stronger. The amplitude of the oscillations is higher than in the baseline case, of about 60,000 Pa. In the other side resonator, position 2, the signal is still in phase to the one in position 1, and the two signals coming from the resonators remain generally similar. In the central detonation chamber, the pressure signal at position 10 is of lower amplitude, as in the baseline case. Also as in the baseline case, the signal is in opposition of phase with respect to the signal in the two resonators. Downstream, at the PDC outlet, in position 7, the static pressure mean value is larger than in the baseline case. Since the inlet total pressure is higher in this case, and the geometry, and, hence, the losses are identical, it results that not all the potential energy stored in the inlet total pressure is converted into kinetic energy in the PDC. This is to be expected, since the PDC design pressure was of 6 bars. The frequency and the amplitude of the pressure oscillations remain similar to the baseline case.

The temperature rise due to shock waves in the PDC is slightly in this case than in the baseline case, due to the higher intensity of the shock waves propagating through the PDC.

It can be concluded that the pressure level in the PDC is proportional to the inlet total pressure. The amplitude of the pressure oscillations increases with the increasing inlet total pressure. The lower inlet total pressure tends to decrease the low frequencies (below 1,000 Hz), and to increase the higher frequencies. The exit Mach number decreases at pressures lower than the design point, but not all the potential energy is converted into kinetic energy for higher pressures. The effect of the inlet total pressure on the mean temperature in the PDC is negligible.

Fig. 7. Pressure signal for baseline configuration under increased inlet pressure.

3.3. Effect of inlet temperature

The geometry was unchanged, and the tests were carried out with under the following conditions:

- Inlet total pressure:608384 Pa (6.004 bar);
- Inlet static pressure: 537107 Pa (5.301 bar);
- Inlet total temperature: 448.75 K (175.60 °C);
- Mass flow rate: 0.644 kg/s;
- Outlet pressure: 102447 Pa (0.998 bar).
- Outlet temperature: 291.91 K (18.76 °C).

The pressure and temperature variations in time are presented, respectively, in Fig. 8 and Fig. 5d.

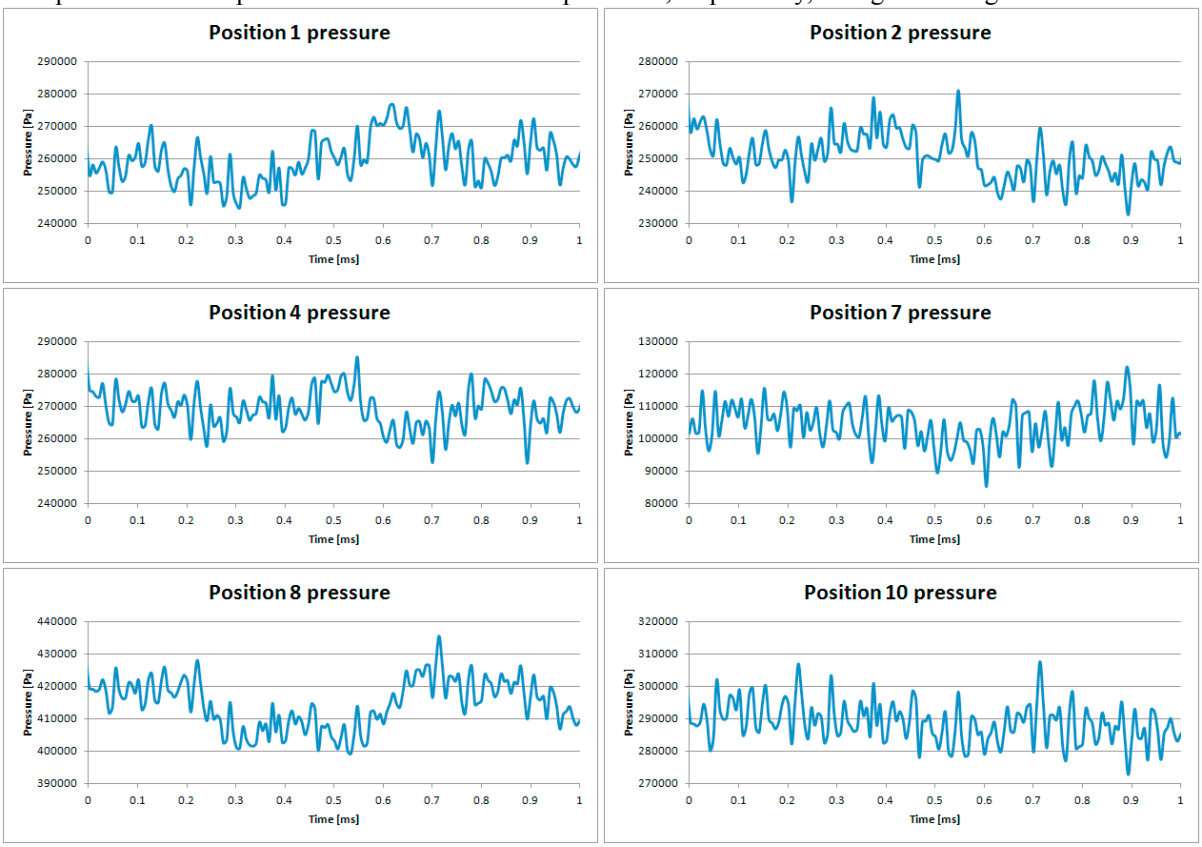

Fig. 8. Pressure signal for baseline configuration under increased inlet temperature.

The static pressure decrease through the Laval nozzle remains visible between the upstream position 8 and the downstream position 4, with about the same value of the difference as for the baseline. The amplitude of the high frequency oscillations is lower than for the baseline, of about 10,000 Pa through the nozzle. The low frequency oscillations have higher amplitudes in position 8 (30,000 Pa) than in position 4, opposite to the baseline situation, indicating an amplification of the pressure waves transmitted upstream through the nozzle. In the resonator placed on the same streamline, in position 1, the data indicates again slightly lower static pressure values, as for the baseline. The amplitudes of both the low and the high frequency pressure oscillations remain lower than in the

baseline case. The higher temperature of the air flowing through the experimental model increases the speed of sound and decreases the flow Mach number, reducing the intensity of the shock waves formed in, and propagating through the experimental model. The pressure signal in the opposite resonator, position 2, is in opposition of phase with the pressure signal in position 1, in correlation with the numerical simulations by Porumbel et al. (2017). In general, the two signals coming from the resonators are similar. In the central detonation chamber, the static pressure in position 10 is higher than in the resonator, indicating a lower velocity. Further downstream in the central detonation chamber, in position 7, the static pressure is again significantly lower than in position 10, but higher than for the baseline. Corroborated with the position 10 data, this shows that at high temperatures, the experimental model fails to fully convert the potential energy of the inlet total pressure into kinetic energy. Both the frequency and the amplitude of the oscillations remain similar to those recorded upstream, in position 10. In general, the intensity of the shock waves in the experimental model and the amplitude of the oscillations are reduced through the effect of the temperature on the speed of sound.

The temperature rise due to shock waves in the PDC is slightly higher in this case than for the baseline (about 17 K), but remains insufficient to trigger the self – ignition of the fuel. A further strengthening of the shock waves inside the experimental model is required, possibly coupled with a further increase of the inlet temperature.

3.4. Effect of critical section

Next, the effect of the size of the critical section of the convergent – divergent nozzles placed at the experimental model inlets was investigated. For this, the detonation chamber was shifted first downstream, and next upstream, to decrease, respectively increase the value of the critical section. The tests were carried out under the conditions described in Table 2.

Table 2. Test conditions for evaluating the effect of the critical section.

Test	A		B	
Inlet total pressure [Pa] / [bar]	607995	6.000	607669	5.995
Inlet static pressure [Pa] / [bar]	534873	5.279	535756	5.288
Inlet total temperature [K] / [°C]	304.34	31.19	301.22	28.07
Mass flow rate [kg/s]	0.813		0.865	
Outlet pressure [Pa] / [bar]	102268	1.009	102172	1.008
Outlet temperature [K] / [°C]	301.95	28.80	302.04	28.89
Critical section [mm^2]	88		132	

3.4.1. Case A - Decreased critical section

The pressure and temperature variations in time are presented, respectively, in Fig. 9 and Fig. 5e. The mean static pressure upstream of the Laval nozzle, in position 8, is lower than for the baseline, indicating a stronger flow acceleration in the channel between the inlet and the Laval nozzle. This is an effect of the downstream shift of the detonation chamber, which also causes a stronger convergence of the channel connecting the PDC inlet to the inlets of the Laval nozzles. At the outlet on the Laval nozzle, in position 4, the mean static pressure is slightly lower than for the baseline, due to the stronger acceleration in the smaller section Laval nozzle. The static pressure drop along the nozzle is slightly lower in this case, of about 120,000 Pa. However, since the inlet velocity is significantly larger here than in the baseline case, the flow acceleration through the supersonic nozzles can be expected to be higher, due to the smaller dimensions in their divergent sections. In the corresponding resonator, in position 1, the mean static pressure is higher, and the amplitude of the oscillations is lower than for the baseline. Nevertheless, the mean static pressure remains lower than at the exit of the Laval nozzle, as in the baseline case. The pressure signal in the opposite side resonator, in position 2, remains in phase with the signal in position 1. As in the other resonator, the amplitude of the pressure oscillations is slightly lower. In position 10, inside the central detonation chamber, the amplitude of the oscillations is lower than for the baseline. The signal is in phase with that coming from the lateral resonators, contrary to the baseline case situation. Finally, in position 7, near the PDC outlet, the mean static

pressure is again substantially lower, and the pressure oscillations are of much smaller amplitudes, as in the case of the baseline configuration. The mean pressure is higher than for the baseline case, indicating a lower exit Mach number, most likely due to the higher total pressure losses induced in upstream of the Laval nozzles by the higher flow velocity.

Fig. 9. Pressure signal for the configuration with decreased critical section.

The temperature increase in the experimental model is much reduced compared to the baseline, of around 10 K. The temperature is below the inlet temperature for a significant time. This is an effect of the flow expansion inside the channel connecting the PDC inlet to the supersonic nozzles. Overall, the amplitude of the temperature oscillations is higher than in the baseline case, of about 25 K.

3.4.2. Case B - Increased critical sections

The pressure and temperature variations in time are presented, respectively, in Fig. 10 and Fig. 5f. The mean static pressure upstream of the Laval nozzle, in position 8, is even lower in this case than in the previous one. This shows that the baseline represents an optimal case, where the velocity at the Laval nozzle inlet and also through its upstream feed channel is the lowest, allowing for minimal losses. The higher nozzle inlet velocity is due to the larger critical section, inducing in the flow a smaller hydraulic resistance downstream of the inlet and providing for a stronger acceleration of the flow prior to the nozzle inlet. At the outlet on the Laval nozzle, in position 4, the mean static pressure is much higher than for the baseline, due to the reduced acceleration induced by the larger minimum section of the nozzle. The static pressure drop along the nozzle is of about only 40,000 Pa. Given the data, the supersonic nature of the jet exiting the Laval nozzle is questionable in this case. The amplitudes of the pressure oscillations along the nozzle are similar to the baseline, but the frequency of the low frequency oscillations appears to be higher. In the corresponding resonator, in position 1, the mean static pressure is even higher, and the amplitude

of the oscillations is again lower than for the baseline. As before, the mean static pressure levels are significantly higher than at the exit of the Laval nozzle, strengthening the doubts about the supersonic nature of the flow in this region, since the shape of the resonator channel is convergent. The pressure signal in the opposite side resonator, in position 2, remains in phase with the signal in position 1. As in the other resonator, the amplitude of the pressure oscillations is slightly higher than for the baseline. In position 10, inside the central detonation chamber, the amplitude of the oscillations remains lower than for the baseline. The signal is in opposition of phase with the lateral resonators signals, similarly to baseline, and contrary to the previous case. Finally, in position 7, near the PDC outlet, the mean static pressure is also substantially lower, and the pressure oscillations are of much smaller amplitudes, as in the baseline case. The mean pressure remains higher than for the baseline, and only slightly lower than in the previous case, indicating a lower exit velocity, due to a reduced acceleration in the Laval nozzle of bigger area.

Fig. 10. Pressure signal for the configuration with increased critical section.

The temperature at the probe location remains below the inlet value over a significant time, but less so than in the previous case. The amplitude of the oscillations is larger than for the baseline, of 25 K.

In conclusion, changing the size of the minimum section of the Laval nozzles tends to increase the pressure in the experimental model and to reduce the pressure oscillations. Significant changes in the regimes of the pressure waves travelling through the experimental model are registered in both cases. For an increased cross-section of the Laval nozzles, the supersonic nature of the flow is questionable. The variation of the size of the Laval nozzle minimal cross – section increases the amplitudes of the temperature wave, slightly more when decreasing it. The temperature remains below the inlet total temperature for extended time periods, more for the reduced cross – section size, such that the global effect is a reduction of the temperature increase in the experimental model.

3.5. Effect of distance to resonator

The next set of measurements was carried out to evaluate the effect of the distance between the exit sections of the convergent – divergent nozzles to the sharp edges of the resonator. For this, the resonator was shifted first downstream, and next upstream, to increase, respectively decrease the distance between the exit sections of the convergent – divergent nozzles to the sharp edges of the resonator. The tests were carried out under the conditions described in Table 3.

Table 3. Test conditions for evaluating the effect of the critical section.

Test	A		B	
Inlet total pressure [Pa] / [bar]	607423	5.995	607817	5.999
Inlet static pressure [Pa] / [bar]	524363	5.175	576851	5.693
Inlet total temperature [K] / [°C]	300.18	27.03	300.13	26.98
Mass flow rate [kg/s]	0.794		0.900	
Outlet pressure [Pa] / [bar]	102007	1.007	101993	1.007
Outlet temperature [K] / [°C]	297.49	24.34	302.10	28.95
Distance from nozzle to resonator [mm]	10		14	

3.5.1. Case A - Decreased distance to resonator

The pressure and temperature variations in time are presented, respectively, in Fig. 11 and Fig. 5g.

Fig. 11. Pressure signal for the configuration with decreased distance to resonator.

The temporal profile of the static pressure upstream of the nozzle, in position 8, remains similar to the baseline, but the mean level is somewhat higher. This is an effect of the increased hydraulic resistance downstream of the Laval nozzle, caused by closing the gap between the nozzle and the resonator. In position 4, corresponding to the outlet of the nozzle, the mean static pressure remains higher than for the baseline, while still significantly lower than position 8. The mean static pressure level is comparable to that registered in the same position for an increased distance to the resonator. Since the nozzle upstream pressure is higher than in both the previous case and the baseline, it results that the velocity at the nozzle outlet is higher than for an increased distance to the resonator, but lower than for the baseline. The static pressure drop along the nozzle is lower than for the baseline, of about 130,000 Pa. The low frequency oscillations are no longer visible. In the corresponding resonator, in position 1, the mean static pressure is higher than both for the baseline and for the case of an increased distance. The small gap between the resonator and the nozzle makes more difficult for the jet to escape from the resonator and increases the static pressure inside. The amplitude of the pressure oscillations is much reduced compared to the baseline, supporting the previous hypothesis. In the opposite side resonator, in position 2, the situation is quite similar. The pressure signal is in phase in the two resonators, as for the baseline case. In position 10, inside the central detonation chamber, the static pressure profile is similar to the baseline, with a slight increase in the mean level. The amplitude of the oscillations is slightly smaller than for the baseline, particularly for the high frequency oscillations. The situation is the same in position 7, towards the PDC outlet, with a pressure signal very similar to the baseline, and slightly smaller oscillation amplitudes. The mean static pressure levels are higher than for the baseline, indicating a lower PDC exit velocity. The exit velocity is lower than for an increased distance to the resonator.

The temperature remains below the inlet temperature over significant time periods. The amplitude of the temperature oscillations is also larger than for the baseline, of about 20 K.

3.5.2. Case B - Increased distance to resonator

The pressure and temperature variations in time are presented, respectively, in Fig. 12 and Fig. 5h.

Upstream of the Laval nozzle, in position 8, the static pressure profile is very similar to the baseline, showing that the position of the resonator inside the experimental model does not affect the flow upstream of the Laval nozzle critical section. At the nozzle exit, in position 4, the mean static pressure is higher than for the baseline, even if it remains significantly lower than the mean static pressure in position 8. This implies a lower nozzle outlet velocity. The static pressure drop along the nozzle is lower than for the baseline, of about 100,000 Pa. In the same side resonator, in position 1, the mean static pressure is higher than for the baseline, while the signal is very similar. A higher static pressure indicates a lower velocity in the resonator. Since the gap between the nozzle exit and the resonator is larger, the core of the jet exiting the nozzle has more space to bypass the resonator and turn towards the central region. In the resonator placed on the other side, in position 2, the pressure signal is very similar, both in mean level and in shape and amplitude of the oscillations. The pressure signal is in phase in the two resonators, as in the baseline case. Inside the central detonation chamber, in position 10, the mean pressure levels are higher than for the baseline case, and the low frequency oscillations amplitude is significantly higher. The velocity is lower in the central detonation chamber, and the shock waves propagating from the central jet core into the central chamber are significantly stronger, which is beneficial for the operation of the PDC. The phase of the pressure signal in the central detonation chamber is opposite to the phase of the signal pressure in the resonators. Finally, in position 7, near the PDC outlet, the mean static pressure is again higher than for the baseline, as a result of a lower velocity at the PDC exit, with a very similar shape.

The temperature increase in the experimental model is much reduced compared to the baseline, of around 5 K, mostly due to the fact that the mean temperature in the experimental model is lower than the inlet total temperature. The relative increase in temperature through the shock waves is, however, of around 20 K, higher than for the baseline configuration, but still insufficient for ignition. The change in the distance between the resonator and the Laval nozzles tends to increase the pressure levels in the experimental model, either when increasing, or when decreasing it, for different reasons. Consequently, the exit velocity form the experimental model is lower than in the baseline, in both cases. For an increase in the distance, the amplitude of the pressure oscillations in the central detonation chamber is significantly increased compared to the baseline. Important, but not so drastic regime changes also occur if the distance is decreased, indicating that this distance is the critical element for the control of the oscillations in the experimental model, and the operation of the PDC.

Fig. 12. Pressure signal for the configuration with increased distance to resonator.

3.6. Effect of jet direction

The last test was carried out to evaluate the effect of the direction of the supersonic jets exiting the two Laval nozzles. For this, the experimental model semi – casings were rotated to increase the angle made by the jets with the experimental model's centerline, at the nozzles exit. The tests were carried out with under the following conditions:

- Inlet total pressure:608076 Pa (6.001 bar);
- Inlet static pressure: 575996 Pa (5.684 bar);
- Inlet total temperature: 292.60 K (19.45 °C);
- Mass flow rate: 0.950 kg/s;
- Outlet pressure: 101176 Pa (0.999 bar).
- Outlet temperature: 291.39 K (18.24 °C).

The pressure and temperature variations in time are presented, respectively, in Fig. 13 and Fig. 5i. At the inlet of the supersonic nozzle, in position 8, the mean static pressure level is only slightly higher than for the baseline case. The amplitude of the high frequency oscillation is lower, but the amplitude of the low frequency oscillations is significantly higher. At the outlet of the supersonic nozzle, in position 4 the amplitude of the oscillations is similar to the baseline case, and the mean static pressure level is higher, due to a smaller nozzle exit velocity. In the resonator on the same side, in position 1, the mean pressure level remains higher than for the baseline case, and the amplitude of the high frequency oscillations is reduced. The high frequency oscillations remain of similar amplitude compared to the baseline case. In the opposite side resonator, in position 2, the pressure signal is similar, but in

opposition of phase with respect to the position 1 signal, contrary to the situation for the baseline. In position 10, in the central detonation chamber, the high frequency oscillations are of reduced amplitude compared to the baseline, but otherwise similar in shape. The mean static pressure is higher than for the baseline; hence the velocity in this case is lower. Finally, further downstream, in position 7, close to the PDC exit, the signal is again similar to the baseline, also with smaller amplitude high frequency pressure oscillations. The mean static pressure is higher than for the baseline, because the sensor is placed upstream of the divergent section of the channel.

Fig. 13: Pressure signal for the configuration with increased jet angle

The temperature rise achieved in the experimental model in this case is the highest of all the tested cases, over 30 K in some time intervals, showing the most promise for achieving fuel self – ignition if higher inlet temperature will be used. However, the mean experimental model temperature in position 4 is lower than the inlet total temperature, which diminishes the advantages this configuration from the standpoint of self – ignition.

4. Conclusions

Experimental measurements of pressure and temperature at high frequency have been carried out in order to assess the optimal PDC configuration. The effect of the inlet pressure and temperature, as well as of three geometrical parameters has been determined. The experiments showed that the amplitude of the pressure oscillations increases with the inlet pressure and decreases with the inlet temperature. The PDC geometry includes three critical parameters: the distance between the exit of the convergent – divergent nozzles that allow the fluid to enter the detonation chamber and the resonators, and the sharp edges of the resonator, and the angle of the incoming supersonic jets with respect to the experimental model centerline. The variation of the critical section area induces significant changes in the regimes of the pressure waves travelling through the experimental model, increasing the

pressure in the experimental model and reducing the pressure oscillations. The change in the distance between the resonator and the Laval nozzles tends to increase the pressure levels in the experimental model. When the distance increases, the amplitude of the oscillations in the central detonation chamber is significantly increased. Important regime changes also occur if the distance between the nozzles exit to the resonator edges is decreased. An increase in the jet angle direction triggers the highest temperature rise, but no configuration provides a temperature high enough to reach the self-ignition temperature of the Hydrogen, contradicting the numerical results presented by Porumbel et al. (2014 and 2017).

Acknowledgements

This work was funded by the European Commission, through the Framework Programme 7 European research project no. 335091 – TIDE

References

T. Cuciuc, C.E. Hritcu, G.G. Ursescu, I. Porumbel, C.F. Cuciumita, 2017, "Valveless Pulsed Detonation Chamber Controlled by Hartmann Oscillators ", CEAS 2017, 16 - 20 Oct., Buch., Romania

J.W. Gregory, 2005, "Development of Fluidic Oscillators as Flow Control Actuators", Ph. D. Thesis, Purdue University, West Lafayette, IN, USA

J. Hartmann, 1919, "About a New Method for Generating Sound Vibrations", Letters of the Royal Danish Academy of Mathematics and Physical Sciences, 1 (13)

J. Hartmann, 1939, "Construction, Performance, and Design of Acoustic Air - Jet Generator", Journal of Scientific Instrumentation, 16, pp. 140 - 149

W.M. Jungowski, 1975, "Some Self Induced Supersonic Flow Oscillations", Progress in Aerospace Science, 18, pp. 151 - 175

J. Kastner, M. Samimy, 2002, "Development and Characterization of Hartman Tube Fluidic Actuators for High - Speed Flow Control", AIAA Journal, 40 (10), pp. 1926 - 1934

K.A. Morch, 1964, "A Theory for the Mode of Operation of the Hatmann Air Jet Generator", Journal of Fluid Mechanics, 20 (1), pp. 141 - 159

I. Porumbel, T. Cuciuc, C.F. Cuciumita, C.E. Hritcu, F.G. Florean, 2014, "Large Eddy Simulation of Non-Reactive Flow in a Pulse Detonation Chamber", Proc. 7th Intl. Conf. on Finite Differences, Finite Elements, Finite Volumes, Boundary Elements (F-and-B '14), Gdansk, Poland

I. Porumbel, B.G. Gherman, I. Malael, V. Dragan, 2017, " Numerical Simulation of Detonation in a Valveless Pulsed Detonation Chamber", CEAS 2017, 16 - 20 Oct., Bucharest, Romania

S. Raghu, G. Raman, 1999, "Miniature Fluidic Devices for Flow Control", FEDSM 99-7526, Proceedings of the ASME Fluids Engineering Division Summer Meeting

G. Raman, S. Khanafseh, A.B. Cain, E. Kerschen, 2004, "Development of High Bandwidth Powered Resonance Tube Actuators with Feedback Control", J. Sound Vibr., 269 (3-5), pp.1031-1062

V. Sarohia, H. L. Back, 1979, "Experimental Investigation of Flow and Heating in a Resonance Tube" 1979, Journal of Fluid Mechanics, 94 (4), pp. 649 - 672

S. Sarpotdar, G. Raman, A.B. Cain, 2005, "Powered Resonance Tubes: Resonance Characteristics and Actuation Signal Directivity", Experiments in Fluids, 39, pp. 1084-1095

M. Samimy, J. Kastner, M. Debiasi, 2002, "Control of a High-Speed Impinging Jet using a Hartmann - Tube based Fluidic Actuator", AIAA-2002-2822, 1st AIAA Flow Control Conference, American Institute for Aeronautics and Astronautics, Saint Louis, MO, USA

T.J.B. Smith, A. Powell, 1964, "Experiments Concerning the Hartmann Whistle", Report 64-42, Department of Engineering, University of California, Los Angeles, USA

G.B. Sobeiraj, A.P. Szumowsky, 1991, "Experimental Investigations of an Underexpanded Jet from a Convergent Nozzle Impinging on a Cavity", J. Sound and Vibrations, 149, pp. 375 - 396

G.J. Sreejith, S. Narayanan, T.J.S. Jothi, K. Srinivasan, 2008, "Studies on conical and cylindrical resonators", Applied Acoustics, 69 (12), pp. 1161–1175